

Wear mechanisms associated with the lubrication of zirconia ceramics in various aqueous solutions

Mitjan Kalin^{a,*}, Goran Dražič^b, Saša Novak^b, Jože Vižintin^a

^a Center for Tribology and Technical Diagnostics, University of Ljubljana, Bogišičeva 8, 1000 Ljubljana, Slovenia

^b Department for Nanostructured Materials, Jožef Stefan Institute, Jamova 39, 1000 Ljubljana, Slovenia

Received 7 July 2004; received in revised form 22 September 2004; accepted 24 October 2004

Available online 7 January 2005

Abstract

The wear and friction behaviours of self-mated zirconia ceramics were investigated with sliding tests in various aqueous solutions using a reciprocating ball-on-flat testing geometry. The surface charge on the native surfaces and the wear debris were “controlled” by varying the pH of the aqueous solution over a wide range, i.e., between 1 and 13. The aim of this investigation was to determine the wear mechanisms via analyses of the wear debris using SEM, XRD and TEM. Significantly different properties were observed, depending on the testing conditions in the different aqueous solutions; and the nature of the wear debris and the native surfaces was also found to depend on the testing conditions. Regions with high and low levels of wear and friction were detected. The wear was found to vary by as much as an order of magnitude with the change in pH, and under the same conditions the friction was observed to change by a factor of two. In the first region, i.e., under very acidic conditions, chemical dissolution was the predominant effect, resulting in low wear and low friction. At higher pH values, more complex processes consisting of a hydrothermal transformation causing bulk zirconia fracture and the formation of tribochemically assisted wear-debris layers, which subsequently spalled, resulted in rough surfaces with very high wear and high friction. Furthermore, the electrochemical effects in this region caused a wear peak to appear at the isoelectric point.

© 2004 Elsevier Ltd. All rights reserved.

Keywords: ZrO₂; Wear resistance; Isoelectric point; Lubrication

1. Introduction

Different types of engineering ceramics, e.g., Al₂O₃, ZrO₂, Si₃N₄ and SiC, exhibit strengths and weaknesses under various loading and lubrication conditions. With the increase in ecological awareness, together with the improvements in the performance of ceramics, the interest in using water to lubricate mechanical systems involving ceramics is growing. However, not all ceramics have the same or even suitable properties under water-lubrication conditions. For example, it is well known that silicon nitride and silicon carbide can provide very low levels of wear and a low coefficient of friction; under certain conditions, even super-low friction

(≈0.002) can be obtained,¹ which has encouraged several researchers to investigate these effects in detail. Tribochemical reactions with the formation of SiO₂ layers and extremely smooth surfaces were often observed, depending on the conditions. These layers can lead to hydrodynamic effects, stress reduction and improved boundary-lubrication properties.^{1–3} However, silicon nitride is currently used mainly in applications that are oil-lubricated, i.e., mainly rolling bearings, because of its non-catastrophic failure mode, but also because of its acceptable oil-lubrication performance under specific conditions and/or carefully selected pre-treatments.^{4–6} On the other hand, silicon carbide has been found to have excellent tribological properties when lubricated with water,^{2,7,8} and in fact it is frequently used in mechanical seals for pumps.

Alumina ceramics also exhibit low wear and moderate friction (≈0.4) when used with water^{9–12} or oil⁵ lubricants.

* Corresponding author. Tel.: +386 1 4771 462; fax: +386 1 4771 469.
E-mail address: mitjan.kalin@ctd.uni-lj.si (M. Kalin).

The tribochemical reactions of alumina with water, resulting in various hydrated layers, were found to be the most important for achieving mild wear conditions, due to their smoothness, stress reduction and improved boundary-lubrication. Primarily because of its low wear, alumina is currently used for mechanical seals, water-tap parts, etc. However, its toughness and fracture reliability are rather low, which limits its more widespread use.¹³ On the other hand, various types of toughened zirconia ceramics possess a much higher fracture toughness and, would therefore, be excellent candidates for applications that require high toughness and high reliability, especially if the wear resistance could be improved.¹⁴ Unfortunately, however, results have shown that zirconia ceramics under water-lubrication conditions exhibit extremely high levels of wear and friction,¹⁵ and so cannot be considered as materials with an acceptable tribological performance.

In our previous investigation involving alumina ceramics, but also in other studies of metal systems,¹⁶ it was found that the tribological performance of materials in “water” (aqueous solutions) does not depend only on the “general” loading conditions, but also very much on the pH and the electrochemical properties of the “water” in which the system is operating. In the case of alumina, huge differences were found in the type of wear debris and tribochemical layers formed on the surfaces and their effects on wear and friction. These were found to change in very narrow regions of pH due to changes in the zeta-potential.^{12,17} Since the effects of these variations were not investigated in detail in the past for zirconia, and as a result of our experience of the significant influence of alumina, we have performed an investigation to assess the tribological behaviour of zirconia ceramics in various aqueous solutions, to determine the mechanisms that are taking place, and to quantify the effects of the zeta-potential and the pH. Particular emphasis was put on an analysis of the wear debris using SEM, TEM and XRD.

2. Experimental

The materials used in our investigation were commercially available TZ-3Y zirconia balls (Tosoh USA Inc., Grove City, OH) and in-house prepared discs made from Alcoa A16.SG powder (Alcoa Corp., Pittsburgh, PA). As-received balls of 10 mm diameter were used in the experiments. These balls have a hardness of 11.6 (± 0.1) GPa and their roughness is better than 0.03 μm . The discs were first ground until they were flat and later polished with a sequence of diamond suspensions of 9, 6, 3 and 1 μm on nylon cloth. The roughness of the discs was measured with a stylus-tip profilometer (T8000, Hommelwerke, GmbH, Germany) and the R_a value was 0.05 (± 0.02) μm . The hardness of the disks was measured with a microhardness tester Leitz (Leitz Miniload 2, Ernst Leitz Wetzlar, GmbH, 6330 Wetzlar, Germany) and was found to be 11.2 (± 0.3) GPa.

The aqueous solutions used in the experiments were prepared with distilled water and HCl or NH_4OH to form either

acidic or alkaline solutions. The solutions were left in air for several hours to stabilize the pH, and minor adjustments to the pre-selected pH were made when necessary. Aqueous solutions with a pH of 0.9, 3.9, 6, 8, 10 and 13 were used in this study.

The wear experiments were performed with a reciprocating-sliding test machine TE 77 (Phoenix Tribology Ltd, Newbury, England) at a constant frequency of 1 Hz and a stroke length of 6.8 mm. The discs were stationary in the test machine, while the counter balls were sliding with a reciprocating motion. The total sliding distance in each test was approximately 100 m, corresponding to 14,400 loading cycles. A load of 50 N was used; this resulted in an initial Hertzian contact pressure of 0.9 GPa. All the experiments were performed at room temperature, i.e., at 21 (± 1 °C). The coefficient of friction was continuously measured throughout every experiment. Each experiment was performed three to six times, and an average value and a standard deviation were calculated to obtain the characteristic wear and friction data.

Prior to every experiment the samples were ultrasonically cleaned for 3 min in ethanol and subsequently dried in a stream of air. The same procedure was repeated with distilled water to remove any possible traces of alcohol from the samples. After the experiments the samples were again cleaned in ethanol, dried in a stream of air and the wear-scars on the balls were measured using an optical microscope (Ernst Leitz Wetzlar, GmbH, 6330 Wetzlar, Germany). The wear-scars were approximated as spherical segments, and a geometrical equation for the volume of each spherical segment was used for the wear–volume calculations.¹⁸ A total of four diameter measurements were made on each wear-scar and the mean of these values was used in the wear–volume calculations. The ball and disc samples were also analysed with a stylus-tip profilometer (T8000, HommelWerke GmbH, Schwinningen, Germany) to assess the topographical characteristics of the worn surfaces. Selected samples from each test condition were sputter coated with gold and examined in the SEM (JEOL T330A, Tokyo, Japan).

After each experiment the wear debris was collected by passing the water solution through a 1- μm filter (Nuclepore Corporation, CA). The wear debris on the filters was examined in the SEM after coating with a layer of gold. In addition, the wear debris generated under selected conditions was also investigated in the TEM. To produce the TEM samples a suspension of wear particles in water, produced during the tribological experiments, was filtered using membrane filtration through a very fine membrane, i.e., 0.2 μm . The membranes were covered with a thin carbon layer using a vacuum-evaporation technique. They were then cut into smaller pieces, placed on porous carbon-coated Cu grids for the TEM examination and dissolved in a chloroform vapour. The samples were examined with a TEM (JEOL 2000 FX, Japan) operated at 200 kV. The chemical composition of the particles was studied using a Link AN-10000 EDXS system (energy-dispersive X-ray spectroscopy) with an ultrathin window Si(Li) detector connected to the TEM.

For selected conditions the wear debris collected after the experiments from the water solutions was dried and then analysed with X-ray powder diffraction (XRD, Philips PV, The Netherlands) using Cu K α radiation. The XRD spectra were collected in the range of 2θ from 20 to 70° (with a step size of 0.04° and a recording speed of one step per second).

The zeta-potential (ZP) was analysed using a commercially available tester ZetaPals (Brookhaven Instr. Corp., USA) with highly diluted suspensions at various pH values. At least five measurements were performed for determining each data point.

3. Results

3.1. Wear data

Fig. 1 shows the wear volume of the ball samples as a function of pH. Two distinctive regions of low and high wear can be observed. At pH 0.9 the wear volume is much lower, about an order of magnitude, than for all the other conditions. The corresponding dimensionless wear coefficient was about 5×10^{-5} . In the region of pH between 3.9 and 13 the wear was significantly higher, and varied by about 30–40% for the different aqueous solutions. The corresponding dimensionless wear coefficient was of the order of 10^{-4} . In this region the highest wear was measured at pH 6 (which was also the highest wear observed in this study) and the lowest at pH 10. The wear data suggest that in the most acidic environment the wear corresponds to an intermediate regime, close to mild wear, whereas for all other pH values the wear was severe.

The coefficient of friction exhibited very similar behaviour to the wear, i.e., it had a lower value in the most acidic environment at pH 0.9, but at pH 3.9 it had quickly reached a plateau of almost constant value where it remained for all the other pH values (see Fig. 2). However, both regions had rather high coefficients of friction: about 0.45 for pH 0.9 and 0.75 for the higher pH values.

The profilometric analyses of the wear traces on the discs were also in agreement with the calculated wear data. From

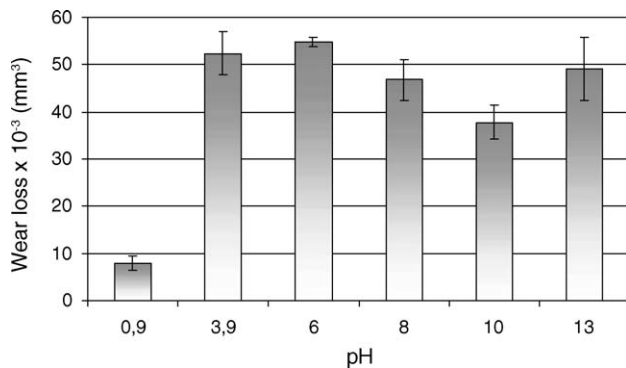


Fig. 1. Wear volume of zirconia pins after 100 m of sliding at 50 N as a function of pH.

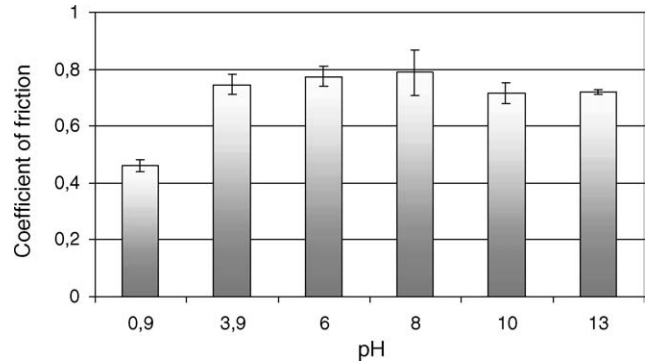


Fig. 2. Steady-state coefficient of friction as a function of pH.

Fig. 3 it is clear that a significantly lower depth of wear trace (about 5 μm) was obtained in the most acidic environment. All the other worn surfaces experienced greater wear depths, from 25 to 35 μm , and the depths also correlated well with the variation in the wear loss. The wear-scar roughness (see the insets in Fig. 3a–f), measured parallel to the sliding direction, indicated very rough worn surfaces in the pH region between 3.9 and 13, having R_a values between 0.16 and 0.25 μm , but a smooth worn surface of 0.02 μm R_a in the case of pH 0.9, which was even smoother than the original un-worn surfaces.

3.2. SEM investigation of the worn surfaces

Fig. 4 shows SEM images of the worn surfaces for various pH values. In agreement with the wear and profilometric results, a clear distinction between the surface at pH 0.9 and all the other surfaces can be seen. The surface at pH 0.9 was extremely smooth and almost featureless (see Fig. 4a). No wear debris or any other signs of any kind of macroscopic damage can be observed. A completely different appearance was found with all the other surfaces (see Fig. 4b–f). The surfaces are covered with layers, obviously consisting of a lot of wear debris, as can be seen at the fractured areas inside the wear-debris layer. However, this debris seems to be bonded together with an amorphous-like phase. Moreover, from the outermost surface of the debris layer in particular, which is at least locally very smooth, it appears that this debris was compacted and substantially smoothed at the interface, as seen from the top, thin tribochemical film with an apparently amorphous appearance (see Fig. 4b–f). These debris layers can be estimated (from the worn surface profilometric measurements) to have a thickness of about 2 μm , and are extensively delaminated and spalled. There is a lot of fracture and deformation found on these layers and a lot of smaller wear debris can also be seen within the fractured pits. The severity of the deformation and spalling is consistent with the very high wear (Fig. 1) measured in this pH region, i.e., between 3.9 and 13.

There is no noticeable difference observed in the wear mechanisms for the surfaces in the high-wear region from pH 3.9 to 13; however, in agreement with the wear (Fig. 1)

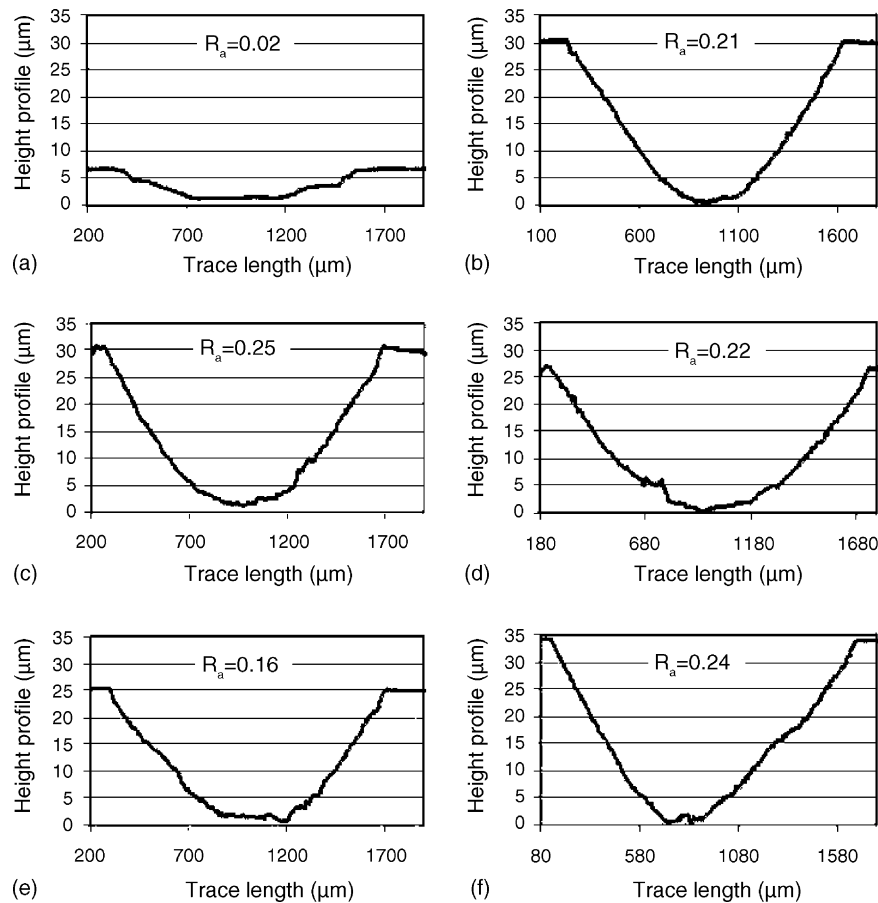


Fig. 3. Comparison of the surface profiles (same vertical scale) of the wear tracks on the discs at a pH of: (a) 0.9, (b) 3.9, (c) 6, (d) 8, (e) 10 and (f) 13. All the trace lengths are 1.7 mm.

and profilometric measurements (Fig. 3), the surface at pH 10 (Fig. 4e) was less damaged, smoother (R_a about $0.16 \mu\text{m}$) and the fracture pits were shallower than for the other surfaces in this region. On the other hand, the surfaces at pH 6 and 13 (Fig. 4c and f), which experienced higher wear, appear to have deeper fracture pits and more severe damage than the surfaces at pH 3.9 and 8 (Fig. 4b and d), and much more than at pH 10, as described before. In agreement with this, also the wear-scar roughness R_a was high for these two conditions: about $0.25 \mu\text{m}$. Moreover, a clearer difference between the surfaces in the high-wear region can be observed at lower magnification, as presented in Fig. 5. It is obvious that the worn surface at pH 6 (Fig. 5a) is much rougher than the surface at pH 10 (Fig. 5b) and exhibits continuous spalling, which agrees very well with the wear results (see Fig. 1).

3.3. SEM investigation of the wear debris

Like with the results presented above, two different types of wear debris that formed during the wear experiments can be distinguished (see Fig. 6). In the very acidic aqueous solutions at pH 0.9 a very small amount of wear debris was collected on the filter (see Fig. 6a). The pieces of debris were mostly separated from each other and rather small, about $1\text{--}3 \mu\text{m}$.

However, at higher magnification some debris at this pH appears to have an amorphous-like form (see Fig. 6b), as observed many times in experiments involving water-lubricated ceramics.^{10,11,19–21} Furthermore, a lot of the wear debris was smaller than $1 \mu\text{m}$ (see Fig. 6b), which is about the same or less than the original grain size of the zirconia used in these experiments, i.e., about $0.3 \mu\text{m}$.

Completely different wear debris was found in the aqueous solutions of all the other pH values. Fig. 6c presents a micrograph of the wear debris collected at pH 6; and for all other conditions in the high-wear region, similar features can be observed. There was always a huge amount of wear debris in the collected water samples, and the pieces had many sizes and shapes: from less than $1 \mu\text{m}$ to more than $30 \mu\text{m}$. Some of the wear debris appears as fractured pieces of bulk zirconia ceramic (see Fig. 6c), but much of the collected debris is delaminated pieces of previously compacted wear-debris tribochemical layers, like that found with the SEM analyses of the worn surfaces (see Fig. 4b–f). Evidence for the mechanism of formation of the compacted layers from fractured and/or tribochemically transformed wear debris through the applied mechanical loads and tribochemically assisted processes during sliding can be seen from the layer presented in Fig. 6d. The observed wear-debris layer is broken into smaller

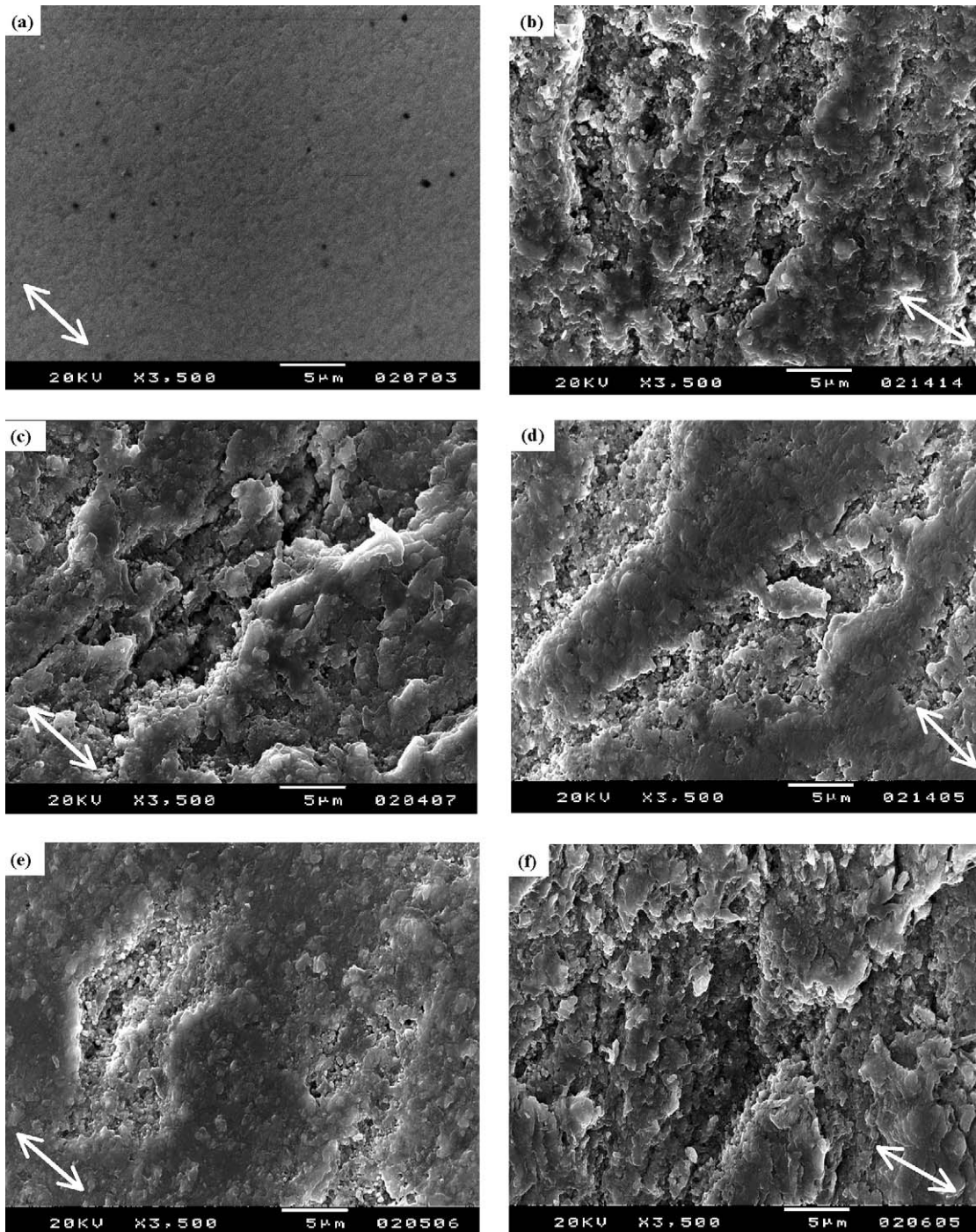


Fig. 4. SEM images of worn surfaces as a function of pH: (a) pH 0.9, (b) pH 3.9, (c) pH 6, (d) pH 8, (e) pH 10 and (f) pH 13. Arrows indicate sliding direction.

pieces of debris, many of them being as small as the zirconia grains (around $0.3 \mu\text{m}$) or smaller. The smoothness and the morphology of this layer suggest that at the sliding interface this debris layer was compacted into a dense and coherent surface top-layer and smoothed via a tribochemical wear mechanism. The process of debris-layer de-cohesion seen in Fig. 6d is probably enhanced by the drying process during sample preparation^{11,22} for the weakly bonded pieces of de-

bris with smaller tribochemically enhanced cohesive forces between them.

3.4. TEM and XRD analyses of the wear debris

A TEM study was only possible for the finest particles (with a thickness less than or equal to 150 nm). The study revealed a quite similar size and shape for the finest wear de-

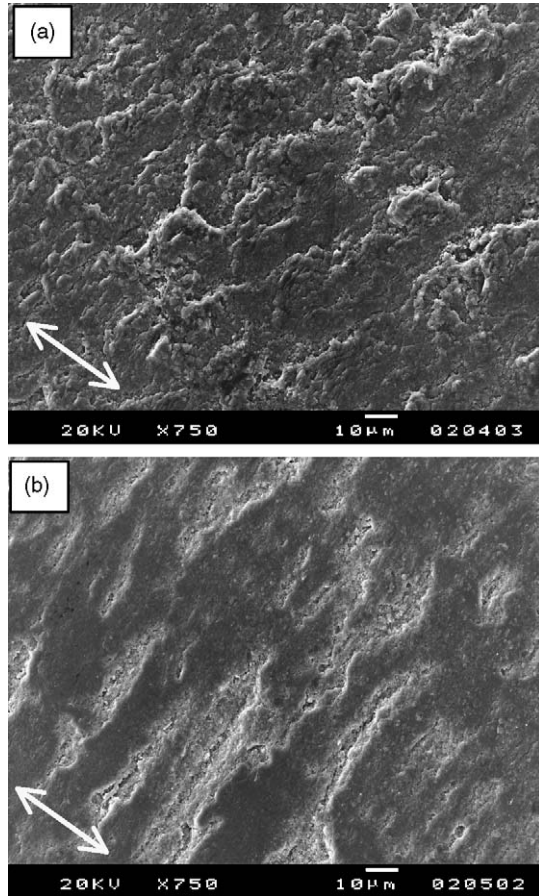


Fig. 5. SEM images of worn surfaces at lower magnification showing macroscopic topographical differences at: (a) pH 6 and (b) pH 10. Arrows indicate sliding direction.

bris generated under different conditions, even in both wear regions, i.e., at pH 0.9 and 6. Their sizes varied from 50 to 500 nm, although these pieces of wear debris were agglomerates. In Fig. 7a a dark-field TEM image of an agglomerate (from the experiment at pH 6) shows the size and morphology of the primary crystalline particles. The primary particles were found to be relatively spherical, with sizes around 3–5 nm. Using the selected-area electron diffraction (SAED) technique, electron diffraction patterns of the primary particles were recorded (see Fig. 7b). The experimental patterns were compared to the calculated (simulated) patterns for various compounds. From the very good fit it was concluded that the primary particles were cubic zirconia, about 3–5 nm in size. A certain amount of amorphous phase between the particles could not be excluded; in fact its presence is very probable. EDXS spectra of the agglomerates showed no other elements besides zirconium and oxygen.

X-ray diffraction (XRD) was used to further characterise the collected wear debris, Fig. 8. The results confirmed that in addition to the tetragonal peaks (denoted as T), which were the only peaks present before the wear experiments (see Fig. 8a), several new peaks were recorded, Fig. 8b. These peaks correspond to a monoclinic zirconia phase (denoted

as M), suggesting that part of the zirconia ceramic subjected to tribological action transformed from the tetragonal to the monoclinic phase, as reported previously for tribological experiments involving zirconia in water²³ or humid air.²⁴ This transformation was reported as a hydrothermal phase transformation, associated with an increase in volume, causing large internal stresses and, as a consequence, stress-corrosion cracking and fracturing²³. The low-intensity of the peaks in the XRD spectrum, shown in Fig. 8b, suggest that part of the collected wear debris was also transformed in the amorphous phase (most probably Zr–OH compounds²⁴), which could correspond to the observed amorphous-like appearance of the worn surfaces and layers of wear debris (see Figs. 4 and 6) and TEM results. Cubic ZrO₂, found in the TEM (see Fig. 7), was not observed in the XRD spectra. The reason for this is most probably the size of the cubic ZrO₂ crystallites (below 5 nm).

4. Discussion

The results of this investigation suggest that the wear of zirconia ceramics can be differentiated into two major wear regions, depending on the pH. The coefficient-of-friction behaviour exactly coincides with these two regions. The first region is at very low pH, i.e., 0.9, and the second at higher pH values, i.e., from 3.9 to 13 (in our investigation). The surfaces at the low pH were very smooth and the wear debris was hard to find because of its small size. Moreover, some of the wear debris appears to be amorphous. These characteristics are clear from the SEM images of the worn surfaces and the wear debris (see Figs. 4a and 6a), but also from the TEM analyses (see Fig. 7). The lowest coefficient of friction and the lowest wear (wear factor in the range of 10^{-5}) under the present conditions suggest that this kind of wear behaviour corresponds to tribochemical wear. The observed tribochemical wear process can be explained by the high solubility of the zirconia at very low pH values. Fig. 9a shows that the solubility is relatively high under these conditions.

In contrast, the high-wear region from pH 3.9 to 13 is characteristic for distinctive thick tribochemical layers (based on profilometric analyses, assumed to be up to 2 μm) that consist of agglomerated wear debris that is compacted together by the applied stress at the interface due to repeated sliding and tribochemical reaction products. The suggested wear process, therefore, consists of several steps. During the initial sliding the local spot-to-spot contact temperature²⁵ at the surface asperities/irregularities increases enough to promote the hydrothermal transformation of zirconia from the tetragonal to the monoclinic phase, as was determined with the XRD analyses (see Fig. 8). This transformation is associated with a volume increase,²³ which causes stress-corrosion cracking and fracturing of the bulk material, resulting in the formation of wear debris and gradually leading to a wear-debris layer. Due to the locally high stresses at the “highest” wear-debris asperities, the debris is further fractured

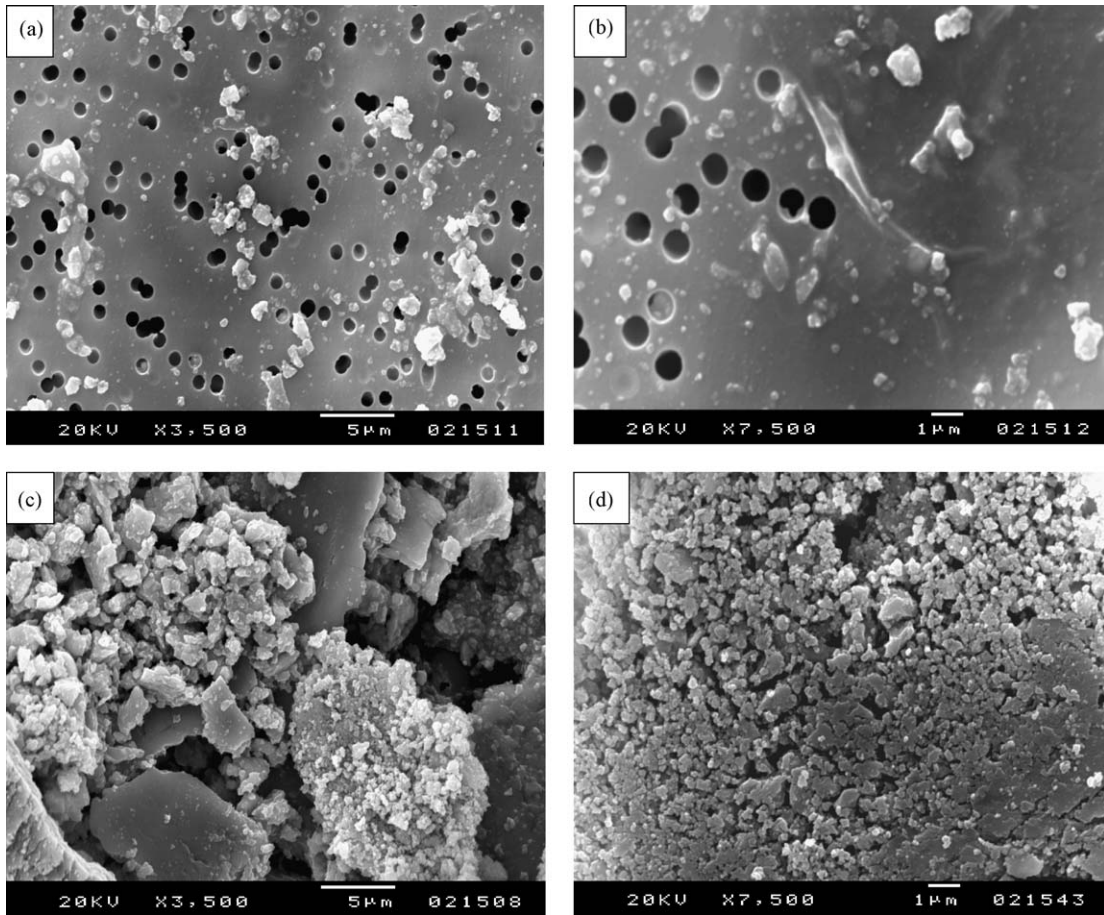


Fig. 6. SEM images of various distinctive types of wear debris at different magnifications as a function of pH: (a and b) pH 0.9 and (c and d) pH 6.

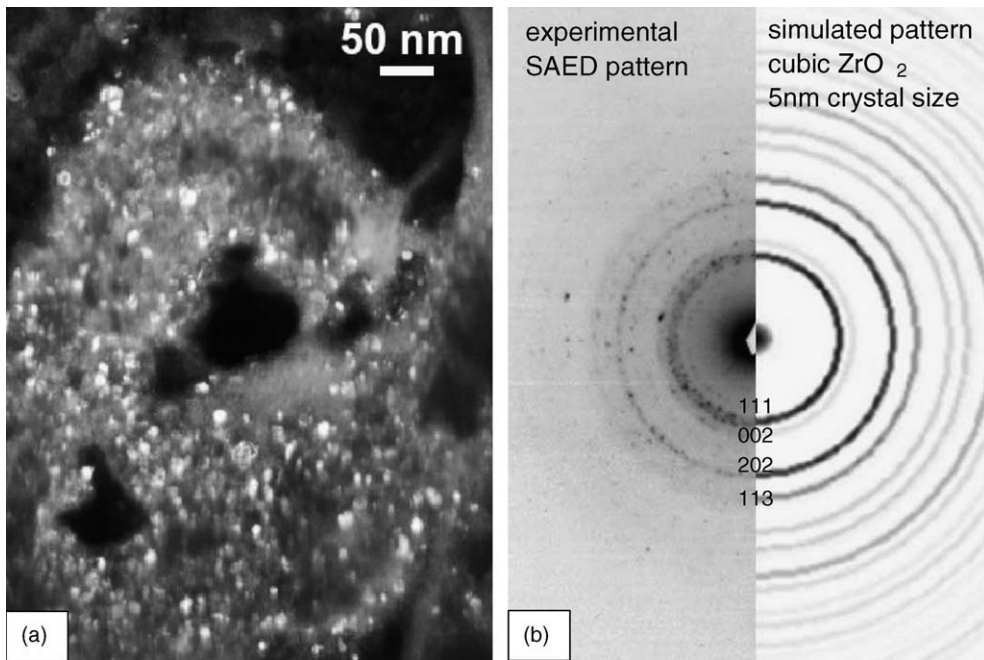


Fig. 7. (a) dark-field TEM image of agglomerate tested at pH 6 consisting of 3–5-nm-sized primary crystalline particles and (b) comparison of experimental and simulated SAED patterns, confirming that the crystalline particles are cubic ZrO₂.

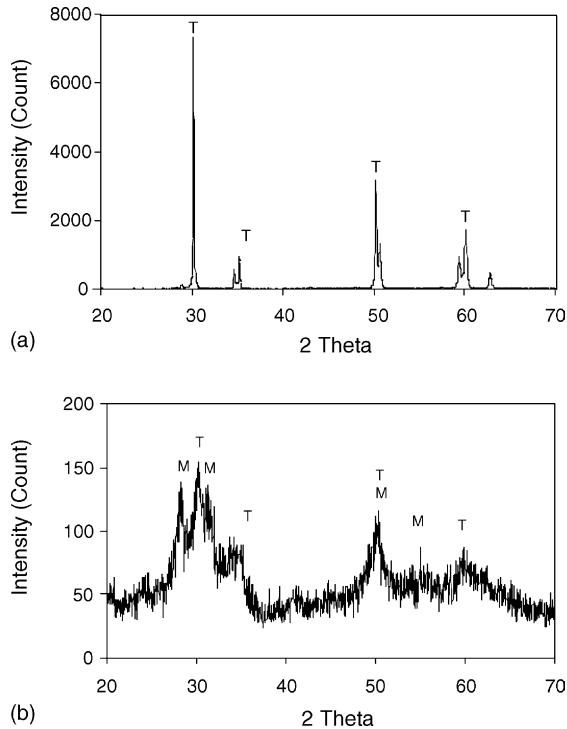


Fig. 8. XRD of (a) un-worn zirconia surface and (b) wear debris collected in the aqueous solution after experiments at pH 6.0. The T-peaks correspond to the tetragonal phase; the M-peaks correspond to the monoclinic phase.

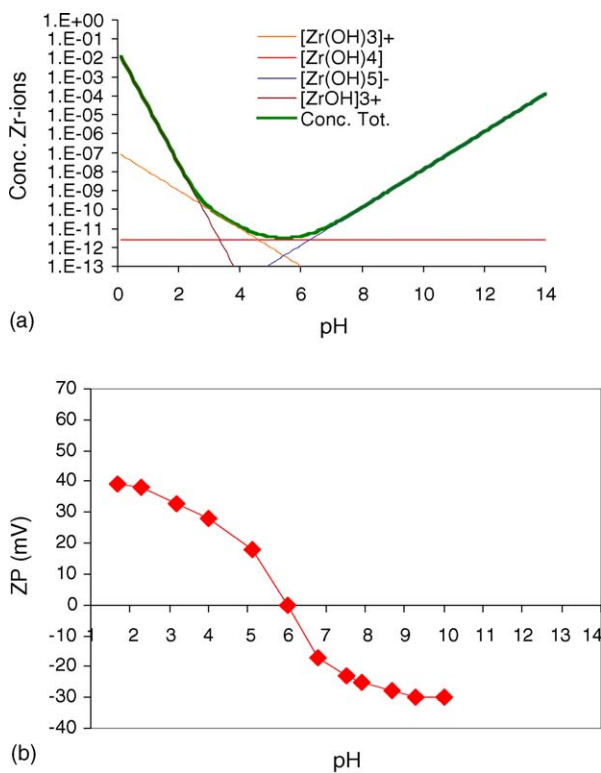


Fig. 9. (a) Solubility and (b) zeta-potential (surface charge) of zirconia as a function of pH.

and/or deformed. At the same time, the tribochemical reaction products are formed by the dissolution and subsequent precipitation of the very small sub-grain, 3–5 nm-size particles, which were observed with the TEM (see Fig. 7). The newly formed particles, together with the larger bulk debris, were covered with an amorphous-type material (most probably Zr–OH compounds²⁴), as observed with the SEM (see Figs. 4 and 6), and supported by the TEM and XRD results. This soft amorphous phase assists in the bonding together of the various debris (from a few nm to a few tens of μm), in particular at the “every-time” sliding surface, and forming a compacted debris layer (see Figs. 4 and 5) as a consequence of the mechanical stresses at the interface and the tribochemically assisted mechanism. The interface was, therefore, rather smooth where it was not fractured, which is typical for a tribochemically assisted processes.^{1,3,19,26} However, due to the substantial influence of the high macro-roughness (see the insets for R_a in Fig. 3) the low friction typical of the smooth tribochemical layers cannot be obtained. This layer is thus seen to form a quasi-static “transition” layer in which the material removed from the layer, either by gradual attrition or sudden detachment, is continually replenished by freshly formed wear debris, causing a high wear factor, of the order of 10^{-4} . Such a high debris-removal rate and the rough surfaces with predominant mechanical wear also caused a high coefficient of friction (Fig. 2), despite the locally smooth tribochemical layer at the interface.

In addition to the above processes, another process needs to be introduced to fully explain the wear behaviour in the high-wear region from pH 3.9 to 13. As seen in Fig. 9b, the zirconia ceramic has its isoelectric point (IEP) where the net surface charge is approximately zero, i.e., at pH 6.0. This condition exactly coincides with the pH where the highest wear was observed in our investigation (see Fig. 1). The increase or decrease in the zeta-potential (ZP), i.e., in the number of positively or negatively charged ions at the native and/or debris surface, results in a change in the wear rate. The same wear mechanism was also observed in our previous studies for alumina ceramics.¹⁷ In this case the mechanism was confirmed by using anionic polyelectrolytes, which allow the zeta-potential to be shifted without a change in the pH value. The wear peaks consistently followed the shift in the IEP.

The effect of the electrochemical potential on the tribological performance of iron and iron oxides in aqueous systems has been described¹⁶ in terms of modifying the normal force via electrostatic repulsion and the surface chemistry, and consequently the shear strength of surface films. The high normal load in our experiments compared to the electrostatic forces does not support the suggestion that the direct changes in the external load are due to a repulsive action. However, the surface chemistry certainly changes, and the resulting repulsive and/or attractive forces modify the nature of the surface layers, primarily affecting the strength of debris agglomeration and compaction, and consequently controlling the coherency, the smoothness and the thickness of the surface tribolayers. With the water-lubrication of alumina these

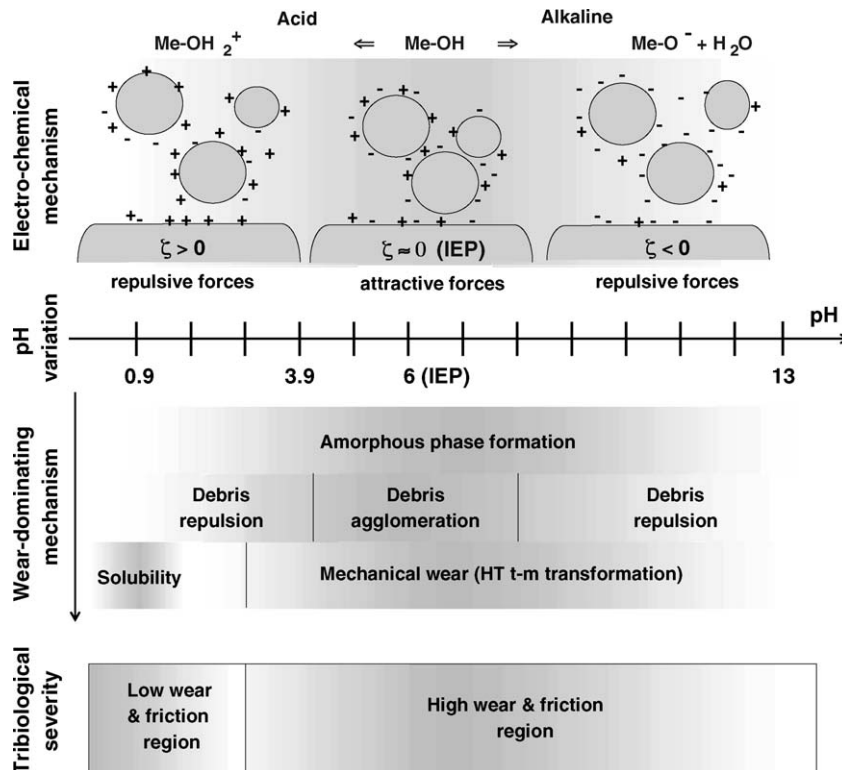


Fig. 10. A schematic illustrating the relations between the electrochemical effects and pH on the mechanisms governing wear behaviour.

changes in the surface layers are more pronounced because of the mild wear,¹² and thus the “wear sensitivity” is higher. On the other hand, due to the predominant effect of the severe mechanical wear of the zirconia in terms of fracture and debris detachment due to the hydrothermal transformation in the pH region from 3.9 to 13, the differences in the nature of the debris films due to electrochemical forces are smaller and relatively less pronounced than in the case of alumina ceramics,^{12,13} where an order-of-magnitude change was observed. Nevertheless, the absolute difference in the specific wear rate for zirconia, depending on zeta-potential, is still very high, about $3.5 \times 10^{-6} \text{ mm}^3/\text{Nm}$. Moreover, clear differences in the roughness, the wear, the coherency and the appearance of the surface tribochemical layers were observed to depend on the surface-charge (zeta-potential) variation also in these experiments involving the water-lubrication of zirconia, as seen in Figs. 4 and 5. A schematic that summarizes the effect of surface charge on electrostatic forces and importance of the observed phenomena on wear mechanisms and “tribological severity” (as a function of pH) in present study is presented in Fig. 10.

5. Conclusions

1. We observed two wear and friction regions, which were dependent on the pH and varied by about an order of magnitude for the wear and by about a factor of two for the friction.
2. In the low-wear region (pH 0.9) the dissolution of zirconia predominates and results in smooth surfaces, a small amount of wear-debris generation, relatively low wear and a low coefficient of friction.
3. In the high-wear region (pH 3.9–13) distinctive tribolayers are formed as a result of the hydrothermal transformation of zirconia, leading to the fracture of the bulk material and the formation of a debris layer. At the same time, the tribochemical reaction products are formed by dissolution and precipitation. The debris is compacted and bonded together by the tribochemical reaction products via mechanical stresses and tribochemically assisted mechanisms. The continuous process of debris-layer removal and freshly formed wear debris caused a very high wear factor, of the order of 10^{-4} . The very rough surfaces under these conditions also cause a high coefficient of friction.
4. The electrochemical potential caused a variation in the degree of agglomeration or repulsion of the wear debris, which, as a consequence, changed the nature of the wear-debris layer. This resulted in significant differences in the wear: the highest being at the isoelectric point (IEP), i.e., at pH 6.
5. Despite the clear and important influence of the electrochemical effects on the formation of debris layer and resulting wear mechanisms, the severe mechanical wear of zirconia (fracture and debris detachment due to hydrothermal transformation) was broadly prevailing wear mechanism in the region of pH from 3.9 to 13. Therefore, the

differences in the nature of the debris films due to electrochemical forces in this region is smaller and relatively less pronounced in comparison to the differences between the solubility-dominated tribochemical wear in the low pH (0.9) region and mechanical wear mechanisms, which dominate in the whole high pH (3.9–13) region.

References

1. Tomozawa, H. and Fischer, T. E., Friction and wear of silicon nitride and silicon carbide in water: hydrodynamic lubrication at low sliding velocity obtained by tribochemical wear. *STLE Trans.*, 1987, **30**, 41–46.
2. Chen, M., Kato, K. and Adachi, K., The comparisons of sliding speed and normal load effect on friction coefficients of self-mated Si₃N₄ and SiC under water lubrication. *Tribol. Int.*, 2002, **35**, 129–135.
3. Xu, J. and Kato, K., Formation of tribochemical layer of ceramics sliding in water and its role for low friction. *Wear*, 2000, **245**, 61–75.
4. Zhao, X.-Z., Liu, J.-J. and Fischer, T. E., Effects of lubricant rheology and additive chemistry in the wear of Si₃N₄ sliding on steel. *Wear*, 1998, **223**, 37–43.
5. Hironaka, S., Boundary lubrication. In *Tribology of Mechanical Systems: a Guide to Present and Future Technologies*, ed. J. Vižintin, M. Kalin, K. Dohda and S. Jahanmir. ASME Press, New York, 2004, pp. 41–51.
6. Kalin, M., Vižintin, J., Novak, S. and Dražič, G., Wear mechanisms in oil-lubricated and dry fretting of silicon nitride against bearing steel contacts. *Wear*, 1997, **210**, 27–38.
7. Hsu, S. M. and Shen, M. C., Ceramic wear maps. *Wear*, 1996, **200**, 154–175.
8. Wang, X. and Kato, K., Improving the anti-seizure ability of SiC seal in water with RIE texturing. *Tribol. Lett.*, 2003, **14**(4), 275–280.
9. Gates, R. S., Hsu, S. M. and Klaus, E. E., Tribochemical mechanism of alumina with water. *Tribol. Trans.*, 1989, **32**(3), 357–363.
10. Andersson, P., Water lubricated pin-on-disc tests with ceramics. *Wear*, 1992, **154**, 37–47.
11. Kalin, M., Jahanmir, S. and Dražič, G., Wear mechanisms of slip-cast glass infiltrated alumina sliding against reference pure alumina in water. *J. Am. Ceram. Soc.*, 2005, **88**(2), 346–352.
12. Kalin, M., Novak, S. and Vižintin, J., Wear and friction behaviour of alumina ceramics in aqueous solutions with different pH. *Wear*, 2003, **254**, 1141–1146.
13. Novak, S. and Kalin, M., The effect of pH on the wear of water-lubricated alumina and zirconia ceramics. *Tribol. Lett.*, 2004, **17**(4), 727–732.
14. Basu, B., Vleugels, J. and Van Der Biest, O., Microstructure–toughness–wear relationship of tetragonal zirconia ceramics. *J. Eur. Ceram. Soc.*, 2004, **24**, 2031–2040.
15. Fisher, T. E., Anderson, M. P., Jahanmir, S. and Slier, R., Friction and wear of tough and brittle zirconia in nitrogen, air, water, hexadecane, and hexadecane containing stearic acid. *Wear*, 1988, **124**(2), 133–148.
16. Zhu, Y. Y., Kelsall, G. H. and Spikes, H. A., The influence of electrochemical potentials on the friction and wear of iron and iron oxides in aqueous systems. *Tribol. Trans.*, 1994, **37**(4), 811–819.
17. Novak, S., Kalin, M. and Kosmač, T., Chemical aspects of wear of alumina ceramics. *Wear*, 2001, **250**, 318–321.
18. ASTM G99, Standard test method for wear testing with a pin-on-disk apparatus. In *Annual Book of ASTM Standards*. 1999, 03.02, p. 401.
19. Jahanmir, S. and Fischer, T. E., Friction and wear of silicon nitride lubricated by humid air, water, hexadecane and hexadecane + 0.5 percent stearic acid. *Tribol. Trans.*, 1989, **32**, 32–43.
20. Takadom, J., Tribological behaviour of alumina sliding on several kinds of materials. *Wear*, 1993, **170**, 285–290.
21. Gee, M. G. and Jennett, N. M., High resolution characterisation of tribochemical films on alumina. *Wear*, 1996, **193**, 133–145.
22. Kalin, M., Hockey, B. and Jahanmir, S., Wear of hydroxyapatite sliding against glass-infiltrated alumina. *J. Mater. Res.*, 2003, **18**(1), 27–36.
23. Hannink, R. H. J., Murray, M. J. and Scott, H. G., Friction and wear of partially stabilized zirconia: basic science and practical applications. *Wear*, 1984, **100**, 355–366.
24. Basu, B., Vitchev, R. G., Vleugels, J., Celis, J. P. and Van Der Biest, O., Influence of humidity on the fretting wear of self-mated tetragonal zirconia ceramics. *Acta Mater.*, 2000, **48**, 2461–2471.
25. Kalin, M., Influence of flash temperatures on the tribological behaviour in low-speed sliding: a review. *Mater. Sci. Eng. A*, 2004, **374**(1), 390–397.
26. Kalin, M. and Jahanmir, S., Influence of roughness on wear transition in glass-infiltrated alumina. *Wear*, 2003, **255**(1/6), 669–676.